

# Experimental Study on Effects of Adipose-Derived Stem Cell–Seeded Silk Fibroin Chitosan Film on Wound Healing of a Diabetic Rat Model

Yan-Yun Wu, MD,\* Yan-Peng Jiao, PhD,† Li-Ling Xiao, MD,\* Min-Min Li, PhD,‡  
Hong-Wei Liu, PhD,\* Sheng-Hong Li, MD,\* Xuan Liao, MD,\* Yong-Tian Chen, MD,\*  
Jiang-Xuan Li, MD,\* and Yang Zhang, MD\*

**Background:** Wound healing is a complex process that relies on growth factors and stimulation of angiogenesis. Tissue engineering materials composed of adipose-derived stem cells (ADSCs) and silk fibroin (SF)/chitosan (CS) may be able to solve this problem. The aim of this study was to investigate the wound-healing potential of ADSC-seeded SF/CS in streptozotocin-induced diabetic rats.

**Materials and Methods:** Thirty-six male Sprague-Dawley rats were purchased and randomly assigned into 3 groups: a control group (no graft), a group treated with SF/CS film graft, and a group treated with ADSC-seeded SF/CS graft. The number of animals in each group was 12. Diabetes was induced by an intraperitoneal injection of streptozotocin. A cutaneous wound was incised at the dorsal region of all the experimental animals. The ADSCs were labeled with CM-Dil fluorescent staining. Wound healing was assessed for all animal groups by observing the rate of wound closure and hematoxylin and eosin staining. The expression of epidermal growth factor, transforming growth factor- $\beta$ , and vascular endothelial growth factor at the wound sites was studied by enzyme-linked immunosorbent assay to evaluate the effect of growth factors secreted by ADSCs. The differentiation of ADSCs was analyzed by immunofluorescence staining.

**Results:** The ADSC-seeded SF/CS film treatment significantly increased the rates of wound closure in treated animals, and hence wound healing was drastically enhanced for ADSC-SF/CS treatment groups compared with control groups and SF/CS film treatment group. Histological observations showed the condition of wound healing. Enzyme-linked immunosorbent assay and immunofluorescence staining observations showed the secretion and differentiation of ADSCs, respectively.

**Conclusions:** Our analyses clearly suggested that it is feasible and effective to enhance wound healing in a diabetic rat model with ADSC-seeded SF/CS film.

**Key Words:** silk fibroin, chitosan, stem cell, wound, diabetes

(*Ann Plast Surg* 2018;80: 572–580)

Received October 12, 2017, and accepted for publication, after revision December 1, 2017. From the \*Department of Plastic Surgery, The First Affiliated Hospital of Jinan University; †Department of Materials Science and Engineering, Jinan University; and ‡Center of Clinical Laboratory Medicine, The First Affiliated Hospital of Jinan University, Guangzhou, China.

Source of funding: Science and Technology Program of Guangzhou, China (201707010267) and Guangzhou Sipintang Biological technology Co., Ltd.

Conflicts of interest: none declared.

Reprints: Li-Ling Xiao, MD, Department of Plastic Surgery, The First Affiliated Hospital of Jinan University, Guangzhou, Guangdong 510632, China. E-mail: xllin@live.cn.

Copyright © 2018 The Author(s). Published by Wolters Kluwer Health, Inc. This is an open-access article distributed under the terms of the Creative Commons Attribution-Non Commercial-No Derivatives License 4.0 (CCBY-NC-ND), where it is permissible to download and share the work provided it is properly cited. The work cannot be changed in any way or used commercially without permission from the journal.

ISSN: 0148-7043/18/8005-0572

DOI: 10.1097/SAP.0000000000001355

Optimum healing of a cutaneous wound requires a well-orchestrated integration of the complex biological and molecular events of cell migration and proliferation, extracellular matrix (ECM) deposition, angiogenesis, and remodeling.<sup>1</sup> Impairment in this orderly progression of the healing process may lead to chronic wounds which often occur in individuals with chronic conditions, such as diabetes.<sup>2</sup> Among the many factors contributing to (nonhealing) chronic wounds are impairment in the production of cytokines by local inflammatory cells, fibroblasts, and reduced angiogenesis are crucial.<sup>1,3</sup> Diminished wound healing is a major complication in diabetes mellitus and can lead to foot ulcers. However, there are limited therapeutic methods to treat this condition.<sup>4</sup>

Tissue engineering is an important therapeutic strategy used in regenerative medicine in the present and in the future. Tissue engineering includes 3 elements: scaffold, growth factors, seed cells. Adipose-derived stem cells (ADSCs) have excellent regenerative capacity, and multiple studies have proven that they augment tissue repairs.<sup>5</sup> Adipose-derived stem cell is rich in soluble factors with paracrine action on fibroblasts and keratinocytes for repair of skin ulcers.<sup>6</sup> Functional biomaterials research is focused on the development and improvement of scaffolding, which can be used to repair or regenerate an organ or tissue. Scaffolds are one of the crucial factors for tissue engineering.<sup>7</sup>

In recent years, silk fibroins (SF), an attractive natural fibrous protein, have good biocompatibility, are safe, have slow degradability, and have remarkable mechanical properties which are proven in many previous studies.<sup>8–11</sup> Silk fibroin has been investigated for surgical implantation, wound healing, and in tissue engineering of bone, cartilage, tendon, and ligament tissues owing to its biocompatibility, relatively low thrombogenicity, relatively low thrombogenicity, low inflammatory response, degradation kinetics, high tensile strength with flexibility, and permeability to oxygen and water.<sup>8,12,13</sup> Silk fibroin in various formats (films, fibers, nets, meshes, membranes, yarns, and sponges) has been shown to support stem cell adhesion, proliferation, and differentiation in vitro and promote tissue repair in vivo.<sup>10</sup>

However, pure SF scaffold is very brittle. The physical properties of SF scaffold can be enhanced by mixing it with other synthetic or natural polymers, such as chitosan (CS) scaffold.<sup>13</sup>

The good potential of CS as a biomaterial derives from its cationic and high-charge density properties, which allow CS to form insoluble ionic complexes with a variety of anionic polymers.<sup>14</sup> Chitosan, is generally inert in vivo and has favorable degradation kinetics and mimics the glycosaminoglycan component of the ECM,<sup>12</sup> has several excellent properties, such as biodegradability, biocompatibility, nonantigenicity, nontoxicity, biofunctional, and antimicrobial properties, which could be beneficial for use in a wide variety of food, agricultural, biotechnological, and pharmaceutical products, such as drug delivery carriers, surgical thread, and bone healing materials.<sup>15,16</sup> In tissue engineering, CS can be generalized to

a variety of soft tissue repairs because it has also been shown to have wound-healing properties, is nontoxic, and has minimal foreign body response with accelerated angiogenesis.<sup>17,18</sup> The blend of SF with CS could facilitate the electrospinning process and allows the well-known structural features of SF to benefit from the surface chemistry of CS to result in a scaffold with features ideal for cell attachment and population of the substratum.<sup>15</sup>

The objectives of our study were, first, to evaluate whether SF/CS could serve as an effective ADSC carrier; second, to understand the impact of ADSC-SF/CS on wound healing; and finally, to study the differentiation potential of transplanted ADSCs in the setting of a diabetic rat cutaneous injury model.

## MATERIALS AND METHODS

### Solation and Culture of ADSCs

Cytological and histological sections were performed in Regenerative Medicine Laboratory of Jinan University for expert assistance in preparing. The rats (Sprague-Dawley) (250–300 g) were anesthetized with 3% pentobarbital sodium (30 mg/kg) and then underwent surgery consisting of a lower abdominal midline incision and bilateral resection of the inguinal fat pads for culture ADSCs. A specimen of inguinal fat was harvested and placed in ice-cold phosphate-buffered saline (PBS). The adipose tissue was rinsed with PBS, minced into small pieces, and then incubated in a solution containing 0.1% collagenase type I (Sigma, St. Louis, MO) for 30 minutes at 37°C with shaking (100 rounds every minute). The top lipid layer was removed, and the remaining liquid portion was centrifuged at 1000g for 10 minutes at room temperature to obtain the stromal cell fraction. The pellet was filtered with a 100- $\mu$ m mesh filter to remove the debris. The filtrate was treated with 0.3% NaCl for 10 minutes to lyse red blood cells and centrifuged at 300g for

10 minutes. The supernatant was discarded, and the remaining cells were suspended in Dulbecco modified Eagle's medium (DMEM) supplemented with 10% fetal bovine serum (FBS) (Hyclone, Logan, Utah), and plated in a 25-cm<sup>2</sup> bottle and cultured at 37°C in 5% CO<sub>2</sub>. The primary cells were cultured for 6 to 7 days until they reached confluence and were defined as "passage 0." Adipose-derived stem cells were cultured and expanded in control medium and used for the experiments at passages 3 to 5.

### Differentiation and Immunophenotyping of ADSCs

Stem cell profile was evaluated through membrane receptor phenotyping and differentiation assays. Stem cell markers were determined through cytometric analysis for CD29, CD45, and CD90 (BD Biosciences, San Jose, CA), FACSCalibur flow cytometer (BD Biosciences). Stem cell pluripotency was evaluated by culture osteogenesis and adipogenesis under specific differentiation medium stimuli. Osteogenesis was induced with low-glucose DMEM supplemented with 10% FBS, dexamethasone (0.1  $\mu$ M), ascorbic acid (0.2 mM), and  $\beta$  glycerol phosphate (10 mM) (Sigma) for 24 days. Adipogenesis was induced with high-glucose DMEM medium supplemented with 10% FBS, dexamethasone (1  $\mu$ M), isobutylmethylxanthine (0.5 mM), insulin (10  $\mu$ g/mL), and indomethacin (100  $\mu$ M) (Sigma) for 18 days. Adipocyte lipid and osteocyte calcium deposits were stained with Oil-red-O and Alizarin Red (Chemicon), respectively.

### Preparation of SF/CS

The blended SF/CS scaffolds were fabricated as described previously, with slight modification.<sup>14,19–21</sup> Briefly, CS was dissolved in 2% acetic acid and clarified by centrifugation. The final concentration of CS used was 2%. Silk cocoons were cut into pieces, degummed (to remove sericin) with a boiling in 0.01 M Na<sub>2</sub>CO<sub>3</sub> solution for 30 minutes,

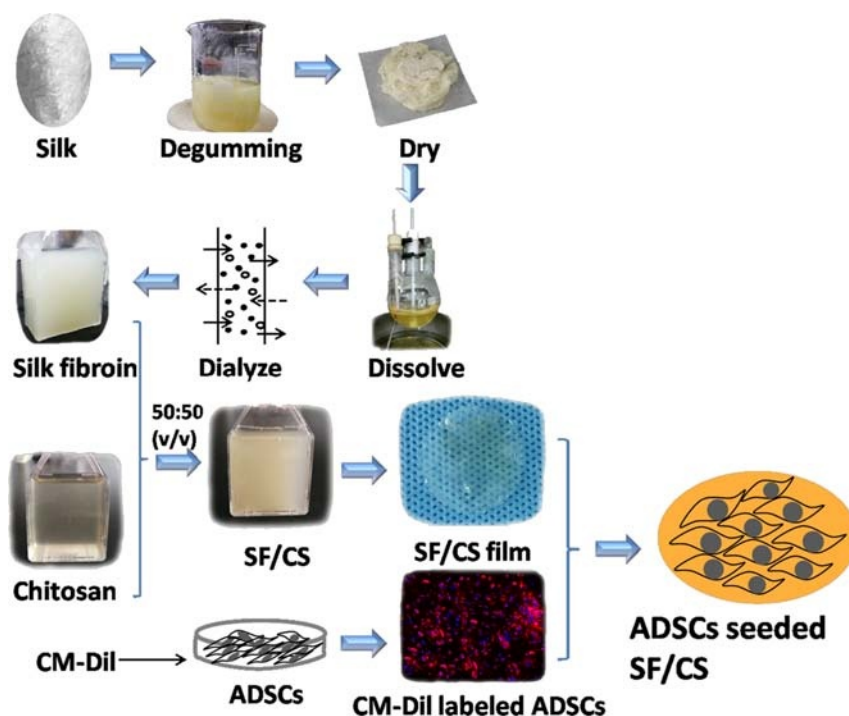


**FIGURE 1.** Flow diagram: the preparation of SF/CS and ADSCs seeded SF/CS. Silk fibroin and chitosan blend (SF/CS) film were cut into 1.5-centimeter-diameter circles before implantation. SF/CS film appears light yellow, transparent and slightly uneven surface. Fluorescence microscope showing immunofluorescence staining of CM-Dil labeled ADSCs (red) in SF/CS film (100 $\times$ ). The nuclei (blue) were then counterstained with 4',6-Diamidino-2-Phenylindole, Dihydrochloride (DAPI).

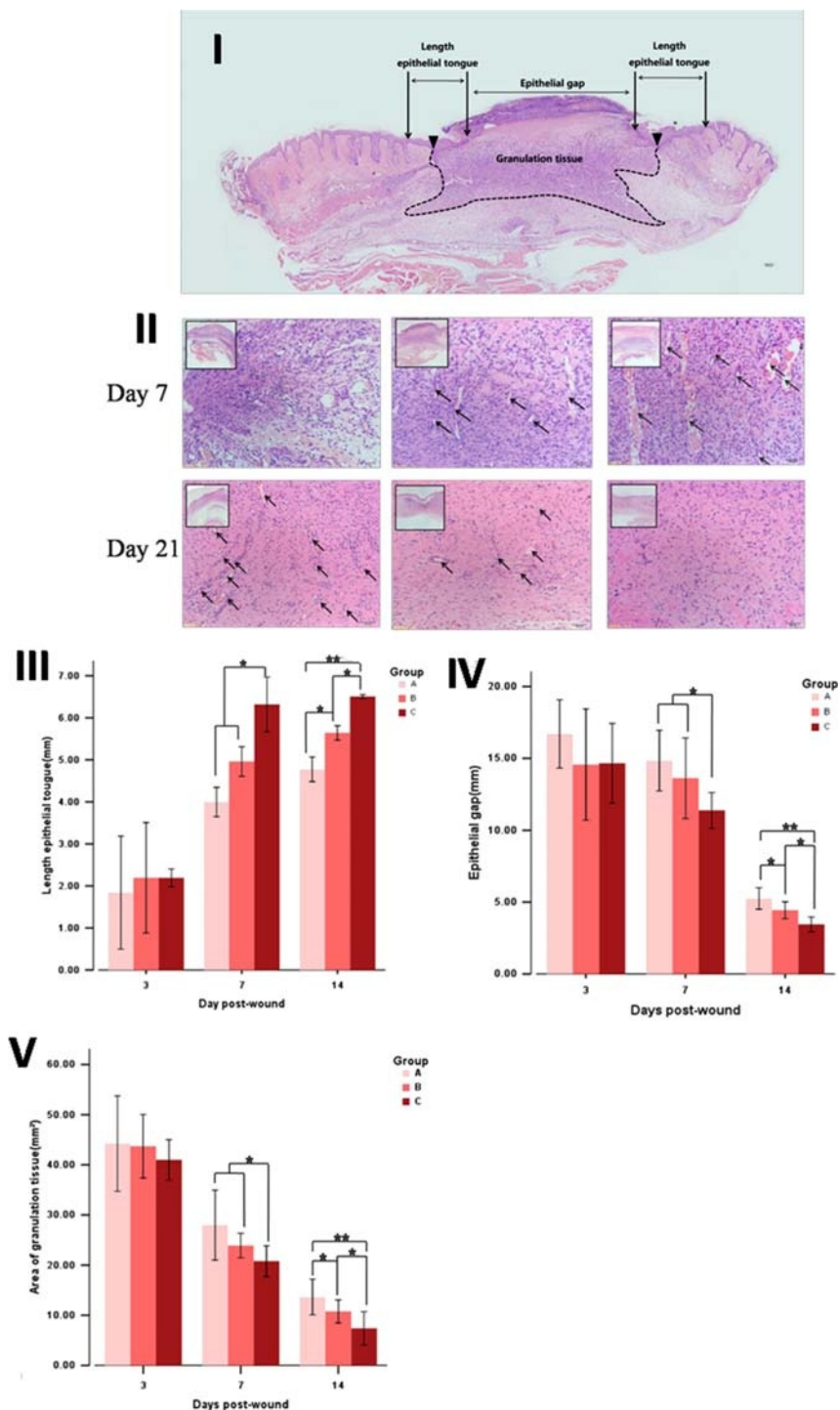


**FIGURE 2.** Histological analysis of skin after hematoxylin and eosin staining. (I) A schematic transversal section is depicted for proper identification of the respective regions observed. (II) Images of granulation tissue were obtained from the healing. The arrows point to the blood vessels (allows) that grow perpendicular to the wound in days 7 and 21 after treatment. Measure and analysis of length epithelial tongue (III), epithelial gap (IV) and area of granulation (V). All data are mean  $\pm$ SD (n = 3). \* $P < 0.05$  ; \*\* $P < 0.01$ .

repeated 3 times, and the fibers were washed with deionized water and then kept at 37°C overnight for drying. The degummed SF was dissolved in calcium nitrate tetrahydrate-methanol solution (molar ratio 1:4:2 calcium/water/methyl alcohol at 80°C), dialyzed against distilled water, and lyophilized to obtain a solid SF fluff. The SF fluff was further

dissolved in distilled water at a 2% (w/v) concentration over a 3-hour period with continuous stirring to obtained aqueous SF solution. The solution was cooled and stored at 4°C until use. A volume of the same concentration of SF was added to prepare a 50:50 (v/v) SF/CS blend and was allowed to mix for 30 minutes (Fig. 1).

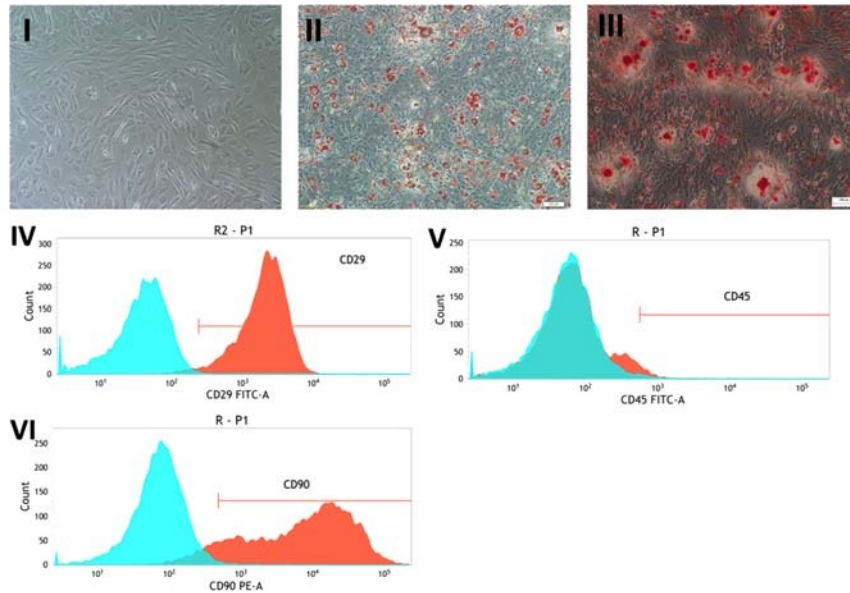


**FIGURE 3.** Culture, Differentiation and Immunophenotyping of ADSCs. (I) Representative image of ADSC displaying cell phenotype under bright-field microscopy (100 $\times$ ). (II-III) Stem cell pluripotency was evaluated by culture adipogenesis and osteogenesis under differentiation stimuli and posterior staining with (II) Oil-red-O and (III) Alizarin Red, respectively (100 $\times$ ). (IV-VI) Immunophenotypic characterization of ADSCs: (IV) CD29 (+), (V) CD45 (-) and (VI) CD90 (-).

### Preparation of ADSC-SF/CS Combination

Adipose-derived stem cells (passage 3) were labeled with CM-Dil, a lipophilic dye that stains the membrane of viable cells. For cell labeling, digested ADSCs were washed with PBS and incubated with CM-Dil (Life

Technologies) in a 37 $^{\circ}$ C incubator for 5 minutes, and then for an additional 15 minutes at 4 $^{\circ}$ C. The cells were washed with PBS twice. The cells were then seeded onto a SF/CS membrane at a density of  $1 \times 10^6$  ADSCs per cm<sup>2</sup>. The cell-seeded SF/CS membrane incubated for 48 hours under standard culture conditions were used for transplantation in animal

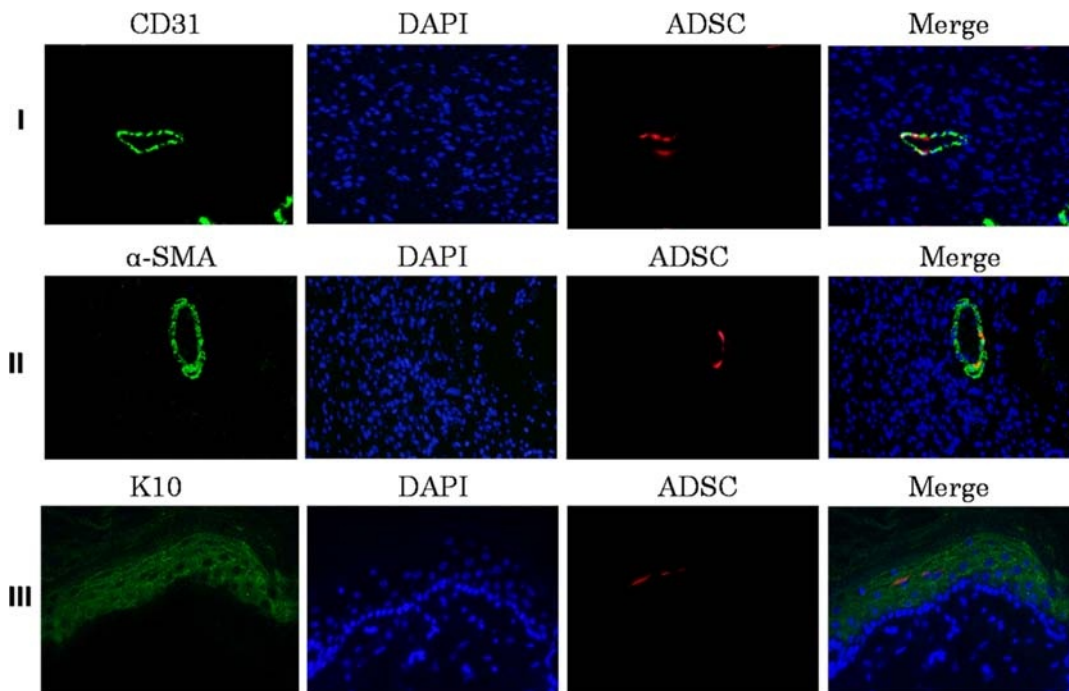


**FIGURE 4.** Expression of epithelial cell markers CD31,  $\alpha$ -SMA, K10 in wound skin. (I) Photomicrographs showing Endothelial cells immunostaining for CD31 (green), engrafted ADSCs (red) in the wound site of diabetic rats, nuclear counterstained with DAPI (blue) at 200 $\times$  magnification. (II) Images showing vascular smooth muscle cells immunostaining for  $\alpha$ -SMA (green), engrafted ADSCs (red) and DAPI (blue) in the wound site of diabetic rats. (III) Images showing epidermal epithelium immunostaining for K10 (green), engrafted ADSCs (red) and DAPI (blue) in the wound site of diabetic rats. Scale bar = 50  $\mu$ m

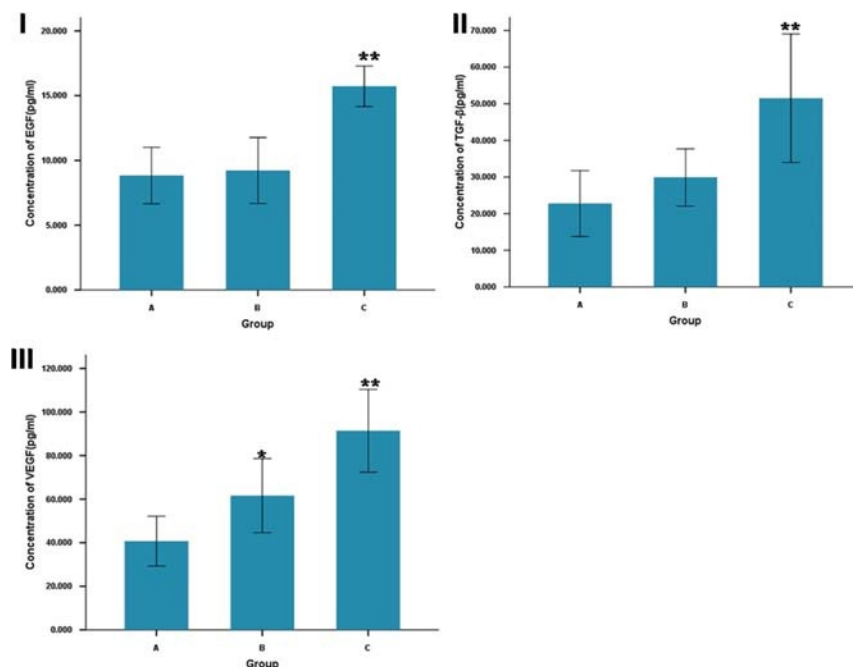


**FIGURE 5.** ELISA analysis of wound tissue for concentration of EGF (I), TGF- $\beta$  (II), and VEGF (III). Comparison of the concentration of Three Growth Factors between ADSC-SF/CS-treated (C), SF/CS-treated (B) and control groups (A) at 14 days post-wound. \*\* $P < 0.01$ , comparison between ADSC-SF/CS-treated and control groups; \* $P < 0.05$ , comparison between ADSC-SF/CS-treated and SF/CS-treated groups.

experiments. Once on the operative field, grafts were transferred to a sterile six-well plate and washed gently in two 500- $\mu$ L aliquots of PBS to remove any nonadherent cells or medium. The cell-seeded SF/CS membrane cultured for 48 hours was observed in a fluorescence microscope (Fig. 1).

### Experimental Diabetes and Excisional Wounding

Experimental animals: 36 male Sprague-Dawley rats (250–300 g) were obtained from Beijing University of Chinese Medicine (Beijing, China). All studies and procedures involving animals were conducted in compliance with guidelines established by the Institute Of Laboratory Animal Science (Jinan University, Guangzhou, China). Rats were kept for 3 weeks on balanced ration with water ad libitum for acclimatization. Standard animal chow and clean water were constantly supplied to the animals.

All procedures complied with the standards stated in the Guide for the Care and Use of Laboratory Animals (Institute of Laboratory Animal Resources, National Academy of Sciences, Bethesda, MD, 1996). Eight-week-old Sprague-Dawley rat received streptozocin 40 mg/kg (Sigma) in 0.05 mol/L citrate buffer, pH 4.5, daily for 5 days. Only mice showing consistent polyuria, polydipsia, polyphagia, weight loss, and elevated blood glucose (>16.7 mmol/L or 250 mg/dL) were included in the study.<sup>22</sup>

These diabetic rats ( $n = 36$ ) were divided into 3 groups with 8 rats in each group randomly: group A, diabetic control with no graft; group B, diabetic treated with SF/CS film alone; and group C, diabetic treated with ADSC-SF/CS. Rats were allowed to manifest hyperglycemia for 8 weeks before surgical wounding. All rats ( $n = 36$ ) were anesthetized with an intraperitoneal injection of sodium pentobarbital (ServiceBio, Inc., Wuhan, China). Their back hair was shaved, carefully. Application field was outlined with marking pen just before removing skin. A 1.5-cm diameter circular impression was made on the middle of dorsum of the mouse. All wounds were cleaned with iodophor and sterile normal saline. Each group received the appropriate

graft as described previously, then were covered with Vaseline oil gauze. Finally, 3M transparent dressing was used to tightly fix the graft and was covered with Vaseline oil gauze.

After completion of wound healing test, rats were sacrificed. Samples of the previously injured tissue were removed at 3, 7, 14, and 21 days. The incision area and adjacent normal skin were excised for each sacrificed animal. Half of every sample fixed in 10% formalin for histological analysis, and the other half was frozen in liquid nitrogen for enzyme-linked immunosorbent assay (ELISA) test.

### Calculation of Wound Healing Rate

Wound closure status was evaluated using a digital camera on days 3, 7, 14, and 21 after treatment. The area of the wound left unhealed was measured using ImageJ software. The wound healing rate was calculated as follows: wound healing rate = (original wound area – wound area on different days postsurgery)/original wound area.

### Histopathological Assay

The sample of skin containing dermis and hypodermis was isolated, carefully trimmed with cutter, and fixed in 10% neutral formalin solution. After paraffin embedding, 3- to 4- $\mu$ m sections were taken and stained with hematoxylin and eosin for study of tissue appearance. Three indices were measured, the length epithelial tongue, the epithelial gap, and the area of granulation tissue as shown in Figure 21. All slides were observed under light microscopic.

### Immunofluorescent Histology

Paraffin-embedded sections first underwent standard deparaffinization and rehydration procedures, and they were then probed with fluorescein isothiocyanate-anti-CD31 antibody (green), anti- $\alpha$ -smooth muscle actin ( $\alpha$ -SMA) antibody (green), anti-cytokeratin 10 antibody (green) (Cell Signaling Technology, Danvers, MA) for overnight at 4°C. Next, sections were incubated with horseradish peroxidase-conjugated secondary antibodies (Santa Cruz Biotechnology Inc., Santa Cruz,

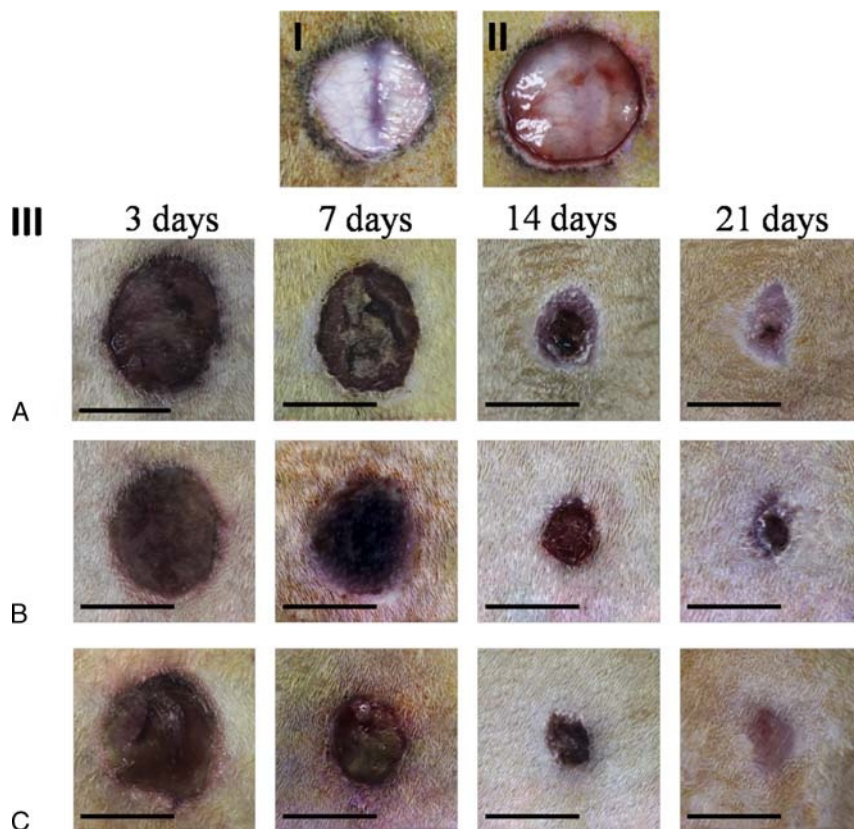


**FIGURE 6.** Macroscopic lesion appearance. Diabetic rats model of skin injury were used (I,III). A standardized wound area (1.5-cm-diameter circle skin in full thickness removed) was induced on the dorsal surface of diabetic rats (I) and normal rats (II) (they have similar weight and age). Compared with normal rats, diabetic rats have poor blood supply, lack of subcutaneous tissue, thin skin and poor elasticity. (III) Lesions appearance at 3, 7, 14 and 21 days.

CA). The nuclei were then counterstained with 4',6-diamidino-2-phenylindole, dihydrochloride.

## ELISA

Weighed, minced samples were placed in lysis buffer containing protease inhibitors for 24 hours at 4°C. Tissues were then homogenized, centrifuged to remove tissue residue, and the amount of epidermal growth factor (EGF), transforming growth factor (TGF)- $\beta$ 1, vascular endothelial growth factor (VEGF) in the lysis buffer was measured in diluted aliquots with standard ELISA assays.

## Statistical Analysis

All data were expressed as means  $\pm$  SD and were analyzed by 1-way ANOVA with Fisher adjustment (SPSS13.0 for windows). Difference between groups was analyzed by Tukey test,  $P$  less than 0.05 was considered statistically significant in all analyses.

## RESULTS

### Characterization of ADSCs

Adipose-derived stem cells were initially expanded for 3 passages and later characterized by cell differentiation and immunophenotyping assays. The cultures were observed by using an inverted light microscope. Attachment of spindle-shaped cells to tissue culture plastic flask was observed after 1 day of culture of ADSCs. Primary cultures reached 70% to 80% confluence in approximately 5 to 6 days. During the passaging, cell growth tended to accelerate and morphology of cells

changed gradually. Cells become more flat-shape with increase in passage number. After 3 passages, cultured cells displayed typical fibroblastoid morphology (Fig. 3I) and under appropriate stimuli, exhibited potential for adipocyte and osteocyte differentiation demonstrated through Oil Red (Fig. 3II), Alizarin red staining (Fig. 3III). Cells also expressed characteristic stem cell markers, CD29 and CD90, and were negative for CD45 (Fig. 3IV–VI).

### Histopathological Assay

Histological examination showed that there was no obvious difference among the 3 groups but significantly higher epithelialization rate, increased granulation tissue formulation, and capillary formation when compared with groups A and B in days 7 and 21 (Fig. 2II). There were more blood vessels (allows), growing perpendicular to the wound, and less inflammatory cell in the wound granulation tissue than the other groups by day 7 (neovascularization,  $A > B > C$ ; inflammatory cell,  $A < B < C$ ). In day 21 after postwound healing, the images showed that the tissue of the wound which was grafted in the ADSCs-SF/CS almost regenerate close to the normal tissue. There still appear some neovascularization, inflammatory cell, and collagen that have not disappeared yet in the 2 other groups, especially control group.

### Immunofluorescent Histology

Engrafted CM-Dil-labeled cells were identified throughout the various substrata of the dermis and cutaneous appendages at 7, 14, 21 days postoperatively (Fig. 4). Engrafted ADSCs were identified, on the basis of red CM-Dil signal, at 14 days, engrafted cells were seen incorporated into winding linear structures consistent with

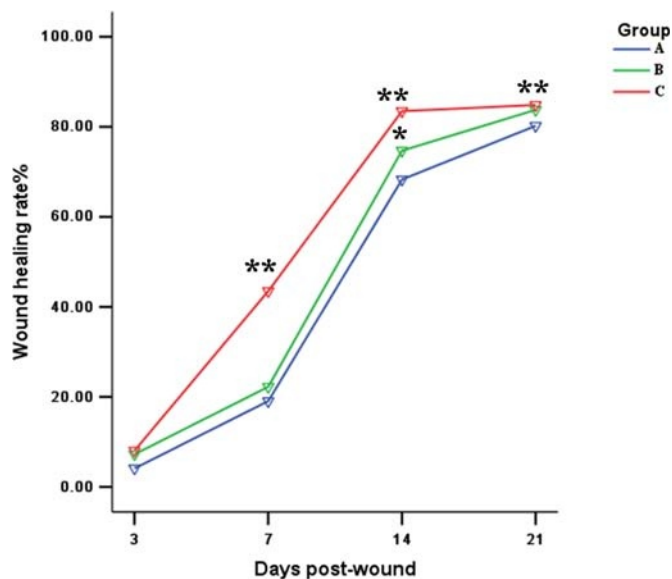


**FIGURE 7.** Analysis of Wound Closure Rates The values were averaged and are reported as mean  $\pm$  SD ( $n=3$ ). \*Significant differences between group B (SF/CS) and group A (control),  $P<0.05$ ; \*\*Significant differences between group C (ADSC-SF/CS) and group A (control) or B (SF/CS),  $P<0.01$ .

microvascular elements and coexpressing positive signals for red CM-Dil and the endothelial marker CD31 (Fig. 4I). Some engrafted ADSCs were noted as recapitulating elements of linear vascular structures, containing for the vascular smooth muscle marker  $\alpha$ -SMA (Fig. 4II) and CM-Dil. However, red fluorescence-labeled cells were not observed to be incorporated into regenerated epidermalepithelium. At 21 days, in addition to these findings described, engrafted Dil-positive cells were observed to be incorporated as components of the regenerated epidermal epithelium on the basis of red fluorescence-labeled cells containing for the cytokeratin marker of epidermal epithelium cytokeratin 10 (Fig. 4III).

## ELISA

Mean EGF, TGF- $\beta$ , and VEGF levels were significantly higher ( $P < 0.01$ ) in ADSCs-SF/CS-treated group compared with SF/CS treated group and controls group at 14 days postoperatively. In addition, mean VEGF levels were higher ( $P < 0.05$ ) in SF/CS-treated group compared with the control group (Fig. 5).

## DISCUSSION

Diabetes is associated with many hemorheological alterations. In diabetic patients, long-term complications are related to the occurrence of vascular alterations which involve hemorheological and endothelium-dependent flow changes, leading to possible tissue ischemia.<sup>23</sup> In this study, based on the comparison between the wound of normal rats and diabetic rats postsurgery immediately (Figs. 6I and II), their skin have some visible changes when they maintain a stable diabetes for 8 weeks, such as poor blood supply, lack of subcutaneous tissue, thin skin, and poor elasticity.

Refractory diabetic wound is a hot and difficult problem. Many studies promoting wound healing by injecting ADSC suspension into wound bed were reported previously.<sup>24,25</sup> However, this method has some unclear security risk. Tissue engineering is an important therapeutic strategy to be used in regenerative medicine in the present and in the future. Therefore, it becomes the best choice for use in tissue engineering to solve this problem.

Tissue engineering includes 3 elements: scaffold, growth factors, and seed cells. Functional biomaterials research is focused on the development and improvement of scaffolding, which can be used to repair or regenerate an organ or tissue. Scaffolds are one of the crucial factors for tissue engineering. Several factors should be considered for developing a device as a skin substitute in tissue engineering, including biocompatibility and safety, degradability, and mechanical properties. Silk fibroin and CS are both natural polymer materials with good biological properties. The advantages of the 2 materials and their positive effects on the wound have been mentioned in this article. After the 2 are blended, they mutually modify each other.<sup>26,27</sup> The SF/CS scaffold has biological, structural and mechanical properties that can be adjusted to meet specific clinical needs.<sup>12</sup> Altman et al<sup>27</sup> concluded that SF/CS is a naturally derived biocompatible scaffold and can be used as a substrate for stem cell delivery. Moreover, their study showed the potential use of SF/CS as a local carrier for autologous stem cells for reconstructive surgery application.

In this study, the same kind of ADSCs was used as seed cells for its potential to secrete of growth factors. ADSCs are easy to obtain and provide a much higher yield.<sup>27</sup> In vitro, ADSCs have been verified that they were able to adhere, proliferate, and migrate to SF scaffolds without affecting their properties. In this study, we seed the CM-Dil-labeled cells onto a SF/CS membrane, cultured for 48 hours, and observed by fluorescence microscope. The surface of SF/CS is uneven, so it is difficult to display all the cells in a plane view but through several plane views. The morphology and the distribution of cells become less uniform because of the uneven surface of SF/CS.

This study successfully used a 50:50 SF/CS blend film, seeded and delivery of ADSCs of the same genus, in a diabetic rat dorsal cutaneous wound model. After a series of experiments and obtaining the data of the relevant test, our finding demonstrates that the construct created by the seeding of ADSCs on SF/CS can be used as an effective delivery vehicle in vivo. Neovascularization and epithelialization were the main reasons behind this process.

Adipose-derived stem cells are a population of pluripotent mesenchymal cells, which can differentiate into various lineages. Adipose-derived stem cells have the potential to promote angiogenesis, secrete growth factors, and differentiate into multiple lineages upon appropriate stimulation.<sup>3</sup> Therefore, in this study, ADSC-seeded SF/CS film can accelerate diabetic wound healing by promoting reepithelialization, cell infiltration, and angiogenesis.

The effects of ADSCs on fibroblasts play a key role in skin biology, such as wound healing, scar, and photoaging. In the early phase of wound healing, fibroblasts migrate into the wound area and move across fibrin-based provisional matrix. Because the provisional fibrin-based matrix is relatively devoid of fibroblasts, the processes of migration, proliferation, and ECM production are the key steps in the regeneration of a functional dermis. Fibroblasts produce collagen-based ECM that ultimately replaces the provisional fibrin-based matrix and help reapproximate wound edges through their contractile properties.<sup>28</sup>

In this study, the contraction of the wound surface was reflected by measuring the length of epithelial crawling and epithelial gap. It can be seen from the histogram that the length of epithelial crawling of ADSC-SF/CS grafted wound is significantly longer than a simple SF/CS grafted wound. This reflects that the fibroblast activity of ADSCs promote wound contraction when analyzed combined with the rate of wound contraction (Figs. 6III and 7).

On the other hand, in line with previous reports, ADSCs promote tissue regeneration through the establishment and support of local microvascular networks.<sup>28,29</sup> According to the development of granulation tissue in hematoxylin and eosin in this study, 7 days after transplantation, the neovascularization of the granulation tissue of wound area in ADSC-SF/CS grafted group was significantly faster than that in the other 2 groups. The blood vessels of the granulation tissue were perpendicular to the wound showing a more mature state. Although there was formation of new blood vessels in the SF/CS grafted wound, this was

less in number and the morphology was relatively immature. Twenty-one days post-wound healing, the ADSC-SF/CS-transplanted wound basically developed to a near normal, and granulation tissue has translated into new skin tissue, and the transplantation of SF/CS group still only has a formation of a few new blood vessels, the control group wound neovascularization, inflammatory cells, and collagen was not reduced. Our findings demonstrate that ADSC plays an important role in promoting angiogenesis and granulation tissue maturation.

Reepithelialization and vascular support in the context of tissue regeneration is likely supported by 2 mechanisms, direct differentiation and through paracrine effectors.<sup>30,31</sup>

Adipose-derived stem cells have excellent regenerative capacity, and multiple studies have proven that they augment tissue repairs. Adipose-derived stem cell is rich in soluble factors with paracrine action on fibroblasts and keratinocytes, such as EGF, fibroblast growth factor, insulin-like growth factor, TGF- $\beta$ , VEGF, and platelet-derived growth factor, important cytokines for repair of skin ulcers. Furthermore, with ADSCs involved in neovascular bed establishment at the site of wound repair, there is likely also an autocrine loop functioning, with local ADSCs producing angiogenic factors that act on themselves or neighboring ADSCs in the reestablishment of vascularization.<sup>6,29,31–33</sup>

In this study, ADSC-SF/CS wound treatment resulted in significantly increased amounts of EGF, TGF- $\beta$ , and VEGF in the wounds. Vascular endothelial growth factor plays a key role in angiogenesis by stimulating endothelial cell proliferation, migration, and organization into tubules. Moreover, VEGF increases circulating endothelial progenitor cells.<sup>30</sup> Transforming growth factor- $\beta$  is a strong stimulator of ECM deposition. EGF promotes the repair and regeneration of damaged epidermis.<sup>34</sup>

High levels of growth factors indicate a paracrine mechanism. Adipose-derived stem cells release wound-healing factors and can stimulate recruitment, migration, and proliferation of endogenous cells in the wound environment. We have shown that ADSCs engrafted via an SF/CS carrier demonstrate spontaneous differentiation into a vascular endothelial phenotype, as evidenced by the colocalization of red fluorescence-labeled ADSC and CD31 staining. Further support for this observation is provided by the observation of red fluorescence DIL/ $\alpha$ -SMA double-positive cells, indicating contribution of a vascular smooth muscle phenotype to the reconstitution of local small vessel matrices. This finding is consistent with previous reports.<sup>31,35</sup> In the present study, we show that ADSCs engraft and differentiate. Immunohistochemistry suggests that the transplanted cells differentiate into vessels, and epithelial phenotypes in their new microenvironment. Consequently, ADSCs can stimulate angiogenesis, epithelialization, and wound remodeling through paracrine secretion and direct differentiation during wound repair.

The functional improvement seen in our study, measured by accelerated rates of wound closure, likely reflects both paracrine and direct cellular mechanisms.

## CONCLUSIONS

In this study, we have successfully applied ADSC-seeded SF/CS as a cytoprothetic hybrid for reconstructive support in a diabetic cutaneous wound healing model which supplies growth factors and promotes angiogenesis of diabetic wound. As a carrier, SF/CS film supports the delivery engraftment and secretion of stem cells, as well as differentiation into vascular and epithelial components. However, there are still some problems and details that have not been resolved, such as the optimum number of cells on the material. In conclusion, ADSC-seeded SF/CS is a promising cell-matrix hybrid and warrants further in vivo study of its potential for reconstructive surgical applications.

## REFERENCES

1. Falanga V. Wound healing and its impairment in the diabetic foot. *Lancet*. 2005; 366:1736–1743.

2. Boulton AJ, Vileikyte L, Ragnarson-Tennvall G, et al. The global burden of diabetic foot disease. *Lancet*. 2005;366:1719–1724.
3. Martin P. Wound healing—aiming for perfect skin regeneration. *Science*. 1997; 276:75–81.
4. Seo E, Lim JS, Jun JB, et al. Exendin-4 in combination with adipose-derived stem cells promotes angiogenesis and improves diabetic wound healing. *J Transl Med*. 2017;15:35.
5. Iyyanki TS, Dunne LW, Zhang Q, et al. Adipose-derived stem-cell-seeded non-cross-linked porcine acellular dermal matrix increases cellular infiltration, vascular infiltration, and mechanical strength of ventral hernia repairs. *Tissue Eng Part A*. 2015;21:475–485.
6. Chen L, Tredget EE, Wu PY, et al. Paracrine factors of mesenchymal stem cells recruit macrophages and endothelial lineage cells and enhance wound healing. *PLoS One*. 2008;3:e1886.
7. Rodriguez-Vazquez M, Vega-Ruiz B, Ramos-Zuniga R, et al. Chitosan and its potential use as a scaffold for tissue engineering in regenerative medicine. *Biomed Res Int*. 2015;2015:821279.
8. Hofmann S, Knecht S, Langer R. Cartilage-like tissue engineering using silk scaffolds and mesenchymal stem cells. *Tissue Eng*. 2006;12:2729–2738.
9. Fernandez-Garcia L, Mari-Buye N, Barrios JA, et al. Safety and tolerability of silk fibroin hydrogels implanted into the mouse brain. *Acta Biomater*. 2016; 45:262–275.
10. Wang Y, Kim HJ, Vunjak-Novakovic G, et al. Stem cell-based tissue engineering with silk biomaterials. *Biomaterials*. 2006;27:6064–6082.
11. Wang P, Deng C, Yuan J, et al. Preparation of antibacterial silk fibroin membranes via tyrosinase-catalyzed coupling of  $\epsilon$ -polylysine. *Biotechnol Appl Biochem*. 2016;63:163–169.
12. Dunne LW, Iyyanki T, Hubenak J, et al. Characterization of dielectrophoresis-aligned nanofibrous silk fibroin-chitosan scaffold and its interactions with endothelial cells for tissue engineering applications. *Acta Biomater*. 2014; 10:3630–3640.
13. Gobin AS, Froude VE, Mathur AB. Structural and mechanical characteristics of silk fibroin and chitosan blend scaffolds for tissue regeneration. *J Biomed Mater Res A*. 2005;74:465–473.
14. She Z, Jin C, Huang Z, et al. Silk fibroin/chitosan scaffold: preparation, characterization, and culture with HepG2 cell. *J Mater Sci Mater Med*. 2008;19:3545–3553.
15. Cai ZX, Mo XM, Zhang KH, et al. Fabrication of chitosan/silk fibroin composite nanofibers for wound-dressing applications. *Int J Mol Sci*. 2010;11:3529–3539.
16. Gobin AS, Butler CE, Mathur AB. Repair and regeneration of the abdominal wall musculofascial defect using silk fibroin-chitosan blend. *Tissue Eng*. 2006;12:3383–3394.
17. Zhang J, Xia W, Liu P, et al. Chitosan modification and pharmaceutical/biomedical applications. *Mar Drugs*. 2010;8:1962–1987.
18. Gu Z, Xie H, Huang C, et al. Preparation of chitosan/silk fibroin blending membrane fixed with alginate dialdehyde for wound dressing. *Int J Biol Macromol*. 2013;58:121–126.
19. Sun K, Li H, Li R, et al. Silk fibroin/collagen and silk fibroin/chitosan blended three-dimensional scaffolds for tissue engineering. *Eur J Orthop Surg Traumatol*. 2015;25:243–249.
20. Deng J, She R, Huang W, et al. A silk fibroin/chitosan scaffold in combination with bone marrow-derived mesenchymal stem cells to repair cartilage defects in the rabbit knee. *J Mater Sci Mater Med*. 2013;24:2037–2046.
21. Zhang XZ, Situ FM, Peng P, et al. Chitosan improves the crystallization of silk fibroin: a three-dimensional scaffold material with better mechanical stability. *Chinese Journal of Tissue Engineering Research*. 2015;19:1858–1863.
22. Gu XY, Shen SE, Huang CF, et al. Effect of activated autologous monocytes/macrophages on wound healing in a rodent model of experimental diabetes. *Diabetes Res Clin Pract*. 2013;102:53–59.
23. Cicco G, Giorgino F, Cicco S. Wound healing in diabetes: hemorheological and microcirculatory aspects. *Adv Exp Med Biol*. 2011;701:263–269.
24. Sheng LL, Yang M, Liang Y, et al. Adipose tissue-derived stem cells (ADSCs) transplantation promotes regeneration of expanded skin using a tissue expansion model. *Wound Repair Regen*. 2013;21:746–754.
25. Karimi H, Soudmand A, Orouji Z, et al. Burn wound healing with injection of adipose-derived stem cells: a mouse model study. *Ann Burns Fire Disasters*. 2014;27:44–49.
26. Zeng S, Liu L, Shi Y, et al. Characterization of silk fibroin/chitosan 3D porous scaffold and in vitro cytology. *PLoS One*. 2015;10:e0128658.
27. Altman AM, Gupta V, Rios CN, et al. Adhesion, migration and mechanics of human adipose-tissue-derived stem cells on silk fibroin-chitosan matrix. *Acta Biomater*. 2010;6:1388–1397.
28. Kim WS, Park BS, Sung JH, et al. Wound healing effect of adipose-derived stem cells: a critical role of secretory factors on human dermal fibroblasts. *J Dermatol Sci*. 2007;48:15–24.

29. Rehman J, Traktuev D, Li J, et al. Secretion of angiogenic and antiapoptotic factors by human adipose stromal cells. *Circulation*. 2004;109:1292–1298.
30. Wu YJ, Chen L, Scott PG, et al. Mesenchymal stem cells enhance wound healing through differentiation and angiogenesis. *Stem Cells*. 2007;25:2648–2659.
31. Altman AM, Matthias N, Yan YS, et al. Dermal matrix as a carrier for in vivo delivery of human adipose-derived stem cells. *Biomaterials*. 2008;29:1431–1442.
32. Hassan WU, Greiser U, Wang W. Role of adipose-derived stem cells in wound healing. *Wound Repair Regen*. 2014;22:313–325.
33. Li JX, Xiao LL, Rao CQ, et al. Comparison of isolation and biological characteristics of adipose-derived stem cells from human and rat. *Journal of Jinan University (Natural Science & Medicine Edition)*. 2015;36:324–329.
34. Haubner F, Ohmann E, Pohl F, et al. Wound healing after radiation therapy: review of the literature. *Radiat Oncol*. 2012;7:162.
35. Altman AM, Yan Y, Matthias N, et al. IFATS collection: Human adipose-derived stem cells seeded on a silk fibroin-chitosan scaffold enhance wound repair in a murine soft tissue injury model. *Stem Cells*. 2009;27:250–258.